



A Combination of Embedded Markov Chain and Binomial Probability As A Tool in Sedimentary Facies Analysis

DJADJANG JEDI SETIADI, IYAN HARYANTO, BUDI MULJANA, and SYAIFUL ALAM

Faculty of Engineering Geology, Padjadjaran University
Jln. Raya Bandung Sumedang Km 21, Jatinangor, Sumedang 45363, Indonesia

Corresponding author: budi.muljana@unpad.ac.id

Manuscript received: September, 14, 2020; revised: November, 10, 2021;
approved: March, 30, 2022; available online: August, 2, 2022

Abstract - The methodology of facies analysis may include statistical examination to establish a local facies model. Without such examination, it is very difficult to predict the facies succession and to interpret the changes in depositional conditions from thick or complex stratigraphic sections. Based on the survey of sedimentary geologic literature in Indonesia, it is suggested that the aforementioned statistical method has relatively seldom been used in Indonesia. Such a situation may reflect a gap in information on the methodology and, accordingly, it seems imperative that there should be a re-exposition of the method. This paper presents a concise exposition of the combination of the embedded Markov Chain and binomial probability as one of the most successful statistical methods which are used in facies analysis. The results of previous studies of The Citalang Formation are used as a case study to illustrate its applications to the real geologic world.

Keywords: Citalang Formation, facies analysis, Markov Chain, binomial probability

© IJOG - 2022.

How to cite this article:

Setiadi, D.J., Haryanto, I., Muljana, B., and Alam, S., 2022. A Combination of Embedded Markov Chain And Binomial Probability As A Tool in Sedimentary Facies Analysis. *Indonesian Journal on Geoscience*, 9 (3), p.291-302. DOI: [10.17014/ijog.9.3.291-302](https://doi.org/10.17014/ijog.9.3.291-302)

INTRODUCTION

Background

Facies analysis is one of the most fundamental and successful methodologies devised by sedimentary geologists to comprehend the stratigraphic records (Miall, 1985; Pirrie, 1998; Dalrymple, 2010). Since the 1990s, methodologies for facies analysis have become an intrinsic part of the broader study of sequence stratigraphy (Catuneanu, 2006; Miall, 2016).

The widely adopted methodology of facies analysis (Figure 1) may include statistical examination of the relationships among all observable

facies in order to establish a local facies model. Without such examination, it is very difficult and sometimes impossible to predict the vertical stratigraphic succession of facies, especially for thick, incomplete, or complex section, and consequently to interpret the changing depositional conditions throughout geologic time.

A casual survey of the sedimentary geologic literature in Indonesia suggests that few studies have proposed a local facies model for the stratigraphic records observable in the country. Such a fact, which may reflect the gap of information on the methodology for establishing a facies model, would hamper a match comparison between the

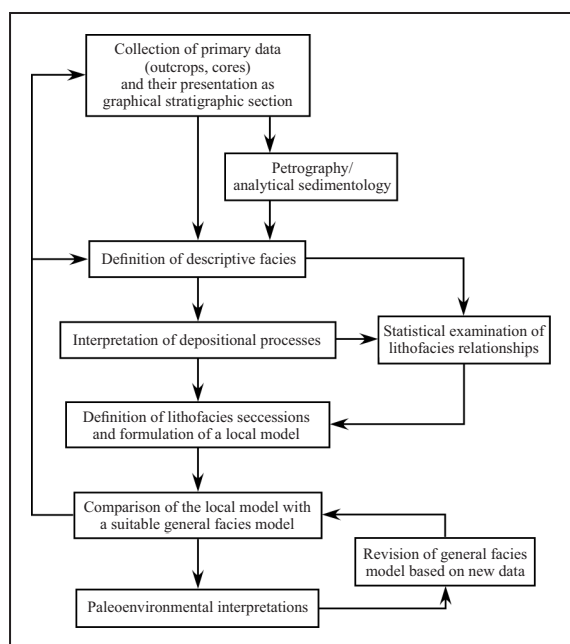


Figure 1. A flow chart of the widely adopted methodology in facies analysis (modified from Miall, 1985 and 2000; Lindholm, 1987).

studied sedimentary rocks and the well known general facies model or other local facies models published in the vast literature of sedimentary geology. Simultaneously, sedimentary researchers in this country may be biased in applying facies models developed in different geologic settings (*e.g.* tectonic environments, geographic milieus, and paleoclimate regimes). It seems imperative, therefore, that there should be a re-exposition of available analytic tools pertaining to the construction of a facies model.

METHODS AND MATERIALS

Methods

This paper presents a concise re-exposition of the methodology of facies analysis with special emphasis on a statistical method, *i.e.* a combination of the embedded Markov Chain and binomial probability that may be used to establish a local facies model. It has been summarized from previous works of Gingerich (1969), Selley (1969), Miall (1973), Cant and Walker (1976), Harper (1984), Lindholm (1987), and Pirrie (1998).

The results of facies analysis of The Citalang Formation (Setiadi, 1998, 2001), with some corrections, will be used in this paper to illustrate the application of the aforementioned methodology. It should be noted, however, that the geology pertaining to the analysis will not be fully presented in this paper. The interested reader is referred to the original contributions for more details on various geologic aspects of the study.

In the last decade, similar Markov Chain approach has been successfully applied in facies analysis of various types of deposits by Stanova *et al.* (2009), Hota and Das (2010), Sumner *et al.* (2012), Colombera *et al.* (2013), Marino and Amaya (2016), Milo (2017), Tewari and Khan (2017), Li *et al.* (2018), Pérez-Pueyo *et al.* (2018), Lapcik (2019), and Subagja *et al.* (2019). As well, this type of approach has been widely used in a wide range of sedimentary deposits, spanning from nonmarine to marine deposits, and in both turbidite and nonturbidite systems. Based on this, not only outcrops data but also borehole logs have been used to describe the facies model, indicating that the Markov Chain method has been successfully applied to both types of data. This method can at the very least reveal a probabilistic model, which can then be used to improve the accuracy of the resulting model by taking into account the characteristics of sedimentary system in the area of interest.

Apart from its traditional applications in palaeoenvironmental analysis, the Markov Chain approach also has recently been developed or combined with other methods to define and characterize hydrocarbon reservoir facies (He *et al.*, 2019; Hsieh *et al.*, 2015; Soto *et al.*, 2014) to analyze the relationship between water depth and carbonate facies (Dyer *et al.*, 2018) to characterize and to predict the distribution of geobodies and subsurface flow units (Croix *et al.*, 2019), and to define soil facies and sequences (Li *et al.*, 2005; Kazi-Tani and Gaouar, 2016).

Materials

The first stage in facies analysis is the collection of primary data, whether in the field at

outcrops or by the examination of cores (Figure 1). The collected data can then be presented as graphic log or graphical stratigraphic sections using a set of standardized symbols to depict the rock types and other lithologic features. Figure 2 shows an example of the presentation of data collected from the Citalang Formation that outcrops discontinuously in the northern part of Sumedang, West Java Province (Figure 3).

On the basis of a predetermined set of objective criteria that can be observed in the field and, subsequently, interpreted in terms of sedimentary process by examining sedimentary geology literature, for example, stratigraphic sections are divided into descriptive lithofacies (Harms *et al.*, 1975; Reineck and Singh, 1980; Scholle *et al.*, 1983; Scholle and Spearing, 1982; Walker, 1984; Walker and James, 1992). Table 1 presents a lithofacies classification scheme for the Citalang Formation (Alam *et al.*, 2019; Setiadi, 1998, 2001); a summary of their interpretation is shown

in Table 2. The methodology was employed in conjunction with the matching sedimentary record found on the Cipelang section as shown in Figure 4.

The next important step in a facies analysis is to establish the facies relationships and succession statistically leading to the formulation of a local facies model. One statistical method that may be employed to do so is a combination of the embedded Markov Chain and binomial probability. The method, which is the central theme of this paper, is going to be described in the next sections.

The last stage of a facies analysis involves a comparison of the local model with a suitable general facies model, and their environmental interpretations are based upon the range of the processes recognized for each of the component lithofacies. The vertical sequence of lithofacies is then interpreted in terms of changing environments or subenvironments of deposition through time. Laterally, equivalent lithofacies associations

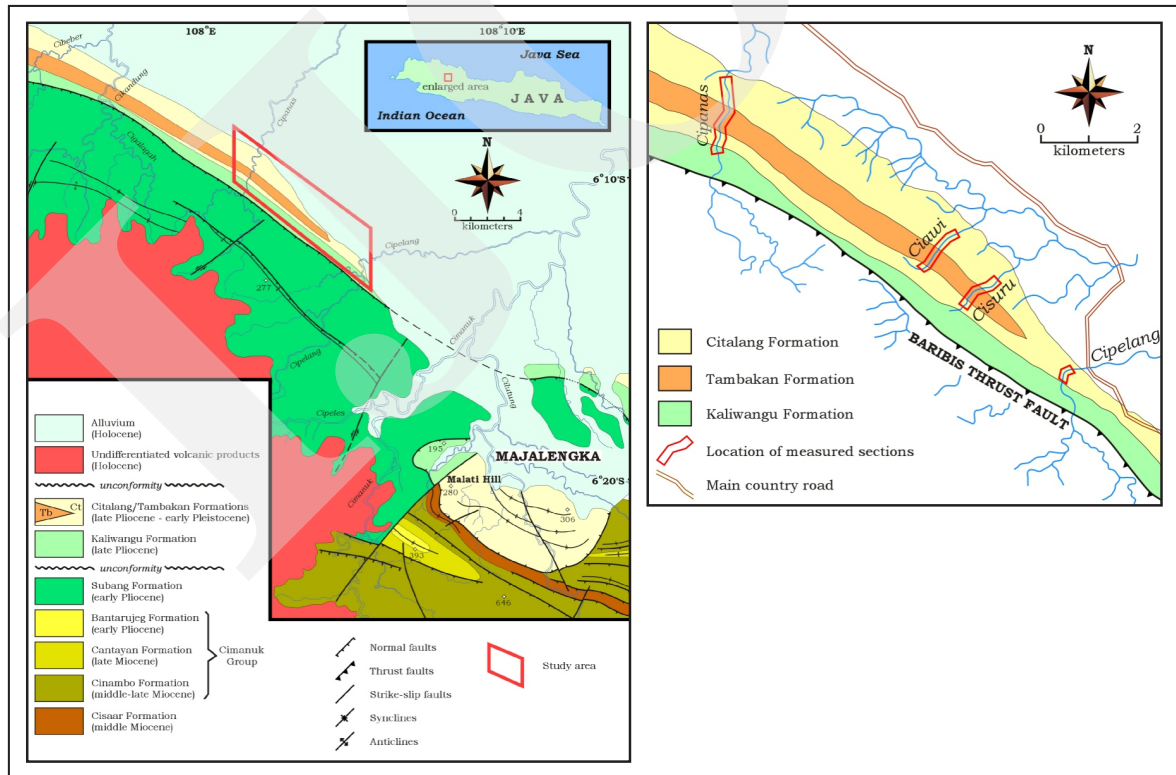


Figure 2. (a) Geologic map showing the distribution of the Citalang Formation in the northern part of the Regency of Sumedang (compiled and modified from Djuri (1973) and Silitonga (1973)). (b). The Location of the Citalang sections measured by Setiadi (1998).

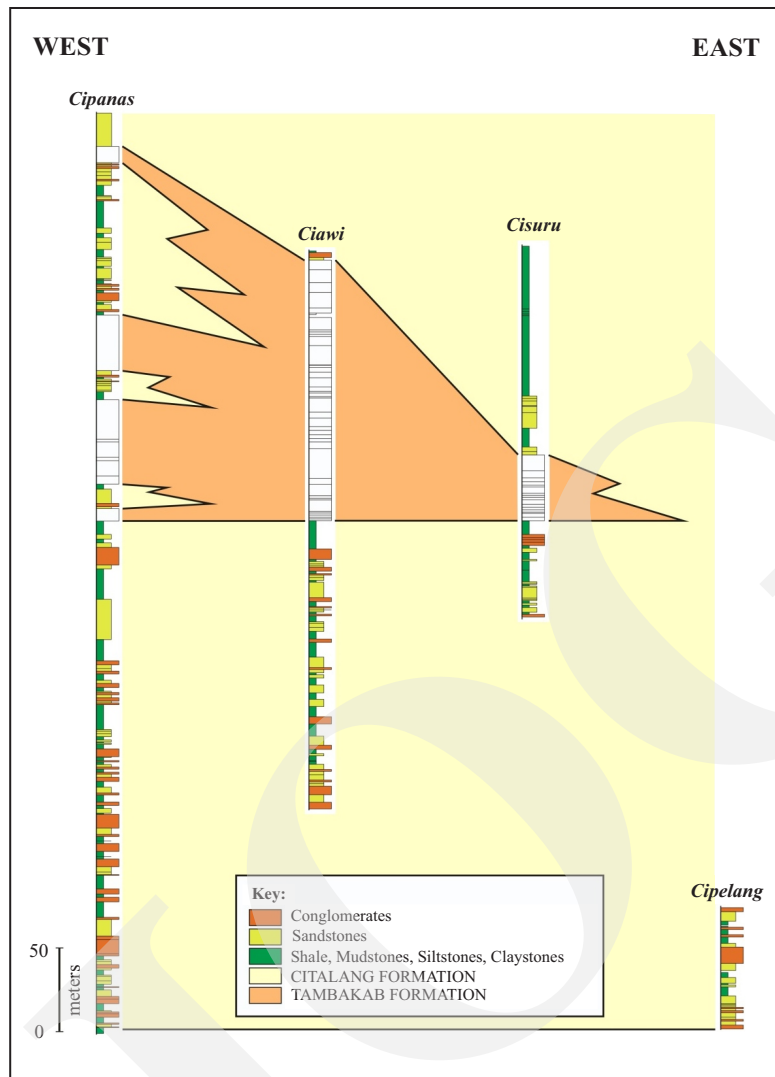


Figure 3. General representation and correlation of the Citalang Formation stratigraphic sections measured in the studied area (Setiadi, 1998).

Tabel 1. Lithofacies Classification in the Studied Area (Setiadi, 1998)

| Facies Code* | Lithofacies | Sedimentary Structures |
|--------------|--|---|
| Gmm | matrix-supported, massive, or crudely bedded conglomerate | crude horizontal bedding, imbrication |
| Gmg | matrix-supported, normal graded conglomerate | graded bedding |
| Gt | trough cross-bedded conglomerate | trough cross-bedding |
| Gp | planar cross-bedded conglomerate | planar cross-bedding |
| Sm | massive sandstone | none |
| Sg | normally graded sandstone | graded bedding |
| Sp | planar cross-bedded sandstone | planar cross-bedding |
| St | trough cross-bedded sandstone | trough cross-bedding |
| Sr | rippled and cross-laminated sandstone | ripple marks of all types and their associated cross-lamination |
| Sh | horizontally laminated sandstone | horizontal lamination |
| Fm | massive mudstone, siltstone, and claystone | none |
| Fl | interlaminated sandstone, mudstone, siltstone, and claystone | fine lamination, very small ripples |

Tabel 2. Summary of the Interpretation of Lithofacies (Setiadi, 1998)

| Facies Code | Sediment Transport and Depositional Processes |
|-------------|--|
| Gmm | debris flows; deposition by "freezing" due to intergranular interaction and cohesion |
| Gmg | gravity flows; deposition from a single current as the energy and flow strength diminished |
| Gt | traction flows; migration of 3-D bars |
| Gp | traction flows; migration of 2-D bars |
| Sm | short-lived mass flows or hyperconcentrated flood-flows; deposition by "freezing" |
| St | traction flows; migration of 3-D ripples or dunes |
| Sp | traction flows; migration of 2-D ripples or dunes |
| Sg | sediment-laden current; deposition was taken place when the current decelerates and the consequent decline in its competence, with coarse grains settling first |
| Sr | waning flood current or traction current at low-water stage |
| Sh | waning flood current or traction current in shallow water; representing the upper plane bed condition, at the transition from subcritical to supercritical flows |
| Fm | suspension fallout |
| Fl | suspension fallout accompanied by periodic input of current transported sands |

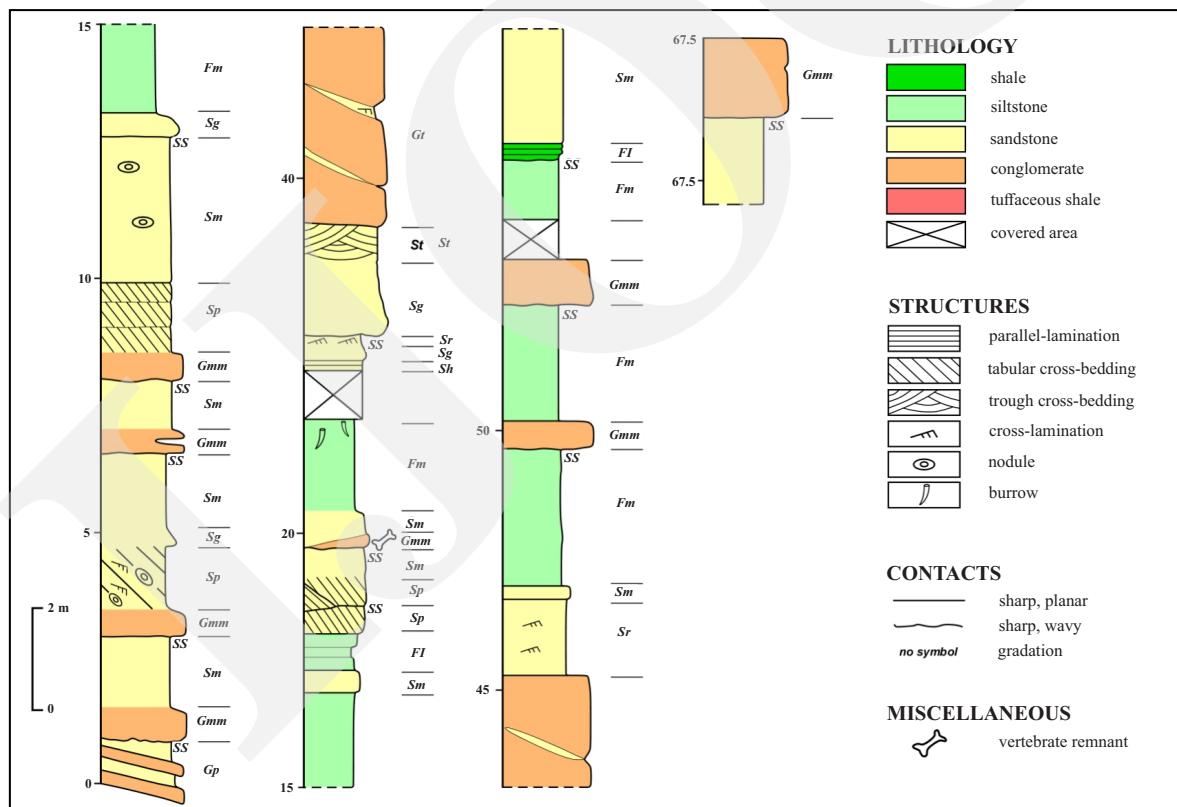


Figure 4. A detailed section of the Citalang Formation and its constituent lithofacies observable on Cipelang River (modified from Setiadi, 1998).

for the same stratigraphical interval may then be interpreted in terms of the spatial distribution of environments for that interval. When appropriate,

therefore, this stage of study may be continued to a depositional system or palaeogeographic analysis.

RESULT AND ANALYSIS

The starting point in the embedded Markov Chain examination in facies analysis is the compilation of a transition count-matrix which tabulates the number of times all possible vertical lithofacies transitions occur in any given stratigraphic succession that has been subdivided into its component facies. Geologically, the table indicates the number of times any one facies passes upward into any other. For example, in Figure 4, the facies Gmm was overlain by the erosional surface (SS) six times and, in turn, was overlain by the facies Sm twice. It should be noted that the second-erosional surface (SS), even though it is not a lithofacies in a normal sense, it is included in the statistics since it marks the discontinuation of a facies transition.

Table 3 is the transition count-matrix which tabulates all facies transitions observable at the Cipanas, Ciawi, Cisuru, and Cipelang sections. Elements in the transition count-matrix are hereafter referred to by the symbol f_{ij} , where i = row number and j = column number.

From the transition count-matrix, two probability matrices may be derived. The first one, the random probability-matrix, consists of elements r_{ij} representing the probability of the given transition occurring randomly. They are given by:

$$r_{ij} = \frac{s_j}{t - s_i} \dots\dots\dots(1)$$

where:

r_{ij} = elements in the random-probability matrix

s_j = the sum of the f_{ij} for the j th column of the matrix

s_i = the sum of the f_{ij} for the i th column of the matrix

t = the total transition

The second one, the transition probability-matrix containing elements p_{ij} , represents the actual probabilities of the given transition occurring in the given section. They are counted using the formula:

$$p_{ij} = \frac{f_{ij}}{s_i} \dots\dots\dots(2)$$

where:

p_{ij} = elements in the transition probability matrix

f_{ij} = elements in transition count matrix

s_i = the sum of the f_{ij} for the i th column of the matrix

Table 3. Transition Count-matrix for the Citalang Formation (Modified from Setiadi, 2001)

| | SS | Gmm | Gmg | Gt | Gp | Sm | Sg | Sp | St | Sr | Sh | Fm | Fl | Row Total |
|--------------|-----|-----|-----|----|----|----|----|----|----|----|----|-----|----|-----------|
| SS | | 57 | 6 | 2 | 9 | 7 | 0 | 2 | 4 | 2 | 0 | 15 | 1 | 105 |
| Gmm | 13 | | 0 | 0 | 0 | 21 | 2 | 7 | 1 | 3 | 0 | 15 | 0 | 62 |
| Gmg | 2 | 0 | | 0 | 0 | 0 | 0 | 0 | 0 | 0 | 0 | 3 | 1 | 6 |
| Gt | 0 | 0 | 0 | | 0 | 1 | 0 | 0 | 0 | 0 | 0 | 1 | 0 | 2 |
| Gp | 2 | 3 | 0 | 0 | | 1 | 0 | 1 | 0 | 0 | 1 | 0 | 1 | 9 |
| Sm | 21 | 0 | 0 | 0 | 0 | | 1 | 5 | 2 | 1 | 2 | 36 | 11 | 79 |
| Sg | 0 | 0 | 0 | 0 | 0 | 2 | | 0 | 0 | 2 | 0 | 2 | 0 | 6 |
| Sp | 6 | 0 | 0 | 0 | 0 | 7 | 0 | | 1 | 1 | 1 | 7 | 1 | 24 |
| St | 1 | 0 | 0 | 0 | 0 | 0 | 0 | 1 | | 0 | 1 | 9 | 0 | 12 |
| Sr | 5 | 0 | 0 | 0 | 0 | 1 | 0 | 1 | 0 | | 3 | 6 | 1 | 17 |
| Sh | 3 | 0 | 0 | 0 | 0 | 3 | 3 | 0 | 1 | 2 | | 1 | 1 | 14 |
| Fm | 38 | 0 | 0 | 0 | 0 | 30 | 0 | 5 | 2 | 4 | 3 | | 19 | 101 |
| Fl | 14 | 0 | 0 | 0 | 0 | 9 | 1 | 1 | 0 | 0 | 0 | 11 | | 36 |
| Column Total | 105 | 60 | 6 | 2 | 9 | 82 | 7 | 23 | 11 | 15 | 11 | 106 | 36 | 473 |

The random probability and transition probability matrices for the observable Citalang facies are presented in Tables 4 and 5.

The last matrix constructed in the Markov Chain analysis is the construction of difference matrix indicating which transitions have occurred with greater than random frequency. The elements of the matrix, d_{ij} , are counted using the equation:

$$d_{ij} = p_{ij} - r_{ij} \dots\dots\dots(3)$$

where:

d_{ij} = elements in the difference matrix

p_{ij} = elements in the transition probability matrix

r_{ij} = elements in the random-probability matrix

Table 6 is the difference matrix for the Citalang facies counted by applying the aforementioned formula to those figures listed in Tables

Table 4. Random Probability Matrix for the Citalang Formation (Modified from Setiadi, 2001)

| | SS | Gmm | Gmg | Gt | Gp | Sm | Sg | Sp | St | Sr | Sh | Fm | Fl | Row Total |
|------------|------|------|------|------|------|------|------|------|------|------|------|------|------|-----------|
| SS | | 0,16 | 0,02 | 0,01 | 0,02 | 0,22 | 0,02 | 0,06 | 0,03 | 0,04 | 0,03 | 0,29 | 0,10 | 1 |
| Gmm | 0,25 | | 0,01 | 0,00 | 0,02 | 0,20 | 0,02 | 0,06 | 0,03 | 0,04 | 0,03 | 0,26 | 0,09 | 1 |
| Gmg | 0,22 | 0,13 | | 0,00 | 0,02 | 0,18 | 0,01 | 0,05 | 0,02 | 0,03 | 0,02 | 0,23 | 0,08 | 1 |
| Gt | 0,22 | 0,13 | 0,01 | | 0,02 | 0,17 | 0,01 | 0,05 | 0,02 | 0,03 | 0,02 | 0,23 | 0,08 | 1 |
| Gp | 0,23 | 0,13 | 0,01 | 0,00 | | 0,18 | 0,02 | 0,05 | 0,02 | 0,03 | 0,02 | 0,23 | 0,08 | 1 |
| Sm | 0,27 | 0,15 | 0,02 | 0,01 | 0,02 | | 0,02 | 0,06 | 0,03 | 0,04 | 0,03 | 0,27 | 0,09 | 1 |
| Sg | 0,23 | 0,13 | 0,01 | 0,00 | 0,02 | 0,18 | | 0,05 | 0,02 | 0,03 | 0,02 | 0,23 | 0,08 | 1 |
| Sp | 0,23 | 0,13 | 0,01 | 0,00 | 0,02 | 0,18 | 0,02 | | 0,02 | 0,03 | 0,02 | 0,24 | 0,08 | 1 |
| St | 0,23 | 0,13 | 0,01 | 0,00 | 0,02 | 0,18 | 0,02 | 0,05 | | 0,03 | 0,02 | 0,23 | 0,08 | 1 |
| Sr | 0,23 | 0,13 | 0,01 | 0,00 | 0,02 | 0,18 | 0,02 | 0,05 | 0,02 | | 0,02 | 0,23 | 0,08 | 1 |
| Sh | 0,23 | 0,13 | 0,01 | 0,00 | 0,02 | 0,18 | 0,02 | 0,05 | 0,02 | 0,03 | | 0,23 | 0,08 | 1 |
| Fm | 0,29 | 0,16 | 0,02 | 0,01 | 0,02 | 0,22 | 0,02 | 0,06 | 0,03 | 0,04 | 0,03 | | 0,10 | 1 |
| Fl | 0,24 | 0,14 | 0,01 | 0,00 | 0,02 | 0,19 | 0,02 | 0,05 | 0,03 | 0,03 | 0,03 | 0,24 | | 1 |

Table 5. Transition Probability Matrix for the Citalang Formation (Modified from Setiadi, 2001)

| | SS | Gmm | Gmg | Gt | Gp | Sm | Sg | Sp | St | Sr | Sh | Fm | Fl | Row Total |
|------------|------|------|------|------|------|------|------|------|------|------|------|------|------|-----------|
| SS | | 0,54 | 0,06 | 0,02 | 0,09 | 0,07 | 0 | 0,02 | 0,04 | 0,02 | 0 | 0,14 | 0,01 | 1 |
| Gmm | 0,21 | | 0 | 0 | 0 | 0,34 | 0,03 | 0,11 | 0,02 | 0,05 | 0 | 0,24 | 0 | 1 |
| Gmg | 0,33 | 0 | | 0 | 0 | 0 | 0 | 0 | 0 | 0 | 0 | 0,50 | 0,17 | 1 |
| Gt | 0 | 0 | 0 | | 0 | 0,50 | 0 | 0 | 0 | 0 | 0 | 0,50 | 0 | 1 |
| Gp | 0,22 | 0,33 | 0 | 0 | | 0,11 | 0 | 0,11 | 0 | 0 | 0,11 | 0 | 0,11 | 1 |
| Sm | 0,27 | 0 | 0 | 0 | 0 | | 0,01 | 0,06 | 0,03 | 0,01 | 0,03 | 0,46 | 0,14 | 1 |
| Sg | 0 | 0 | 0 | 0 | 0 | 0,33 | | 0 | 0 | 0,33 | 0 | 0,33 | 0 | 1 |
| Sp | 0,25 | 0 | 0 | 0 | 0 | 0,29 | 0 | | 0,04 | 0,04 | 0,04 | 0,29 | 0,04 | 1 |
| St | 0,08 | 0 | 0 | 0 | 0 | 0 | 0 | 0,08 | | 0 | 0,08 | 0,75 | 0 | 1 |
| Sr | 0,29 | 0 | 0 | 0 | 0 | 0,06 | 0 | 0,06 | 0 | | 0,18 | 0,35 | 0,06 | 1 |
| Sh | 0,21 | 0 | 0 | 0 | 0 | 0,21 | 0,21 | 0 | 0,07 | 0,14 | | 0,07 | 0,07 | 1 |
| Fm | 0,38 | 0 | 0 | 0 | 0 | 0,30 | 0 | 0,05 | 0,02 | 0,04 | 0,03 | | 0,19 | 1 |
| Fl | 0,39 | 0 | 0 | 0 | 0 | 0,25 | 0,03 | 0,03 | 0 | 0 | 0 | 0,31 | | 1 |

Table 6. Difference Matrix for the Citalang Formation (Modified from Setiadi, 2001)

| | SS | Gmm | Gmg | Gt | Gp | Sm | Sg | Sp | St | Sr | Sh | Fm | Fl | Row Total |
|-----|-------|-------|-------|-------|-------|-------|-------|-------|-------|-------|-------|-------|-------|-----------|
| SS | | 0,38 | 0,04 | 0,01 | 0,06 | -0,16 | -0,02 | -0,04 | 0,01 | -0,02 | -0,03 | -0,15 | -0,09 | 0 |
| Gmm | -0,04 | | -0,01 | 0,00 | -0,02 | 0,14 | 0,02 | 0,06 | -0,01 | 0,01 | -0,03 | -0,01 | -0,09 | 0 |
| Gmg | 0,11 | -0,13 | | 0,00 | -0,02 | -0,18 | -0,01 | -0,05 | -0,02 | -0,03 | -0,02 | 0,27 | 0,09 | 0 |
| Gt | -0,22 | -0,13 | -0,01 | | -0,02 | 0,33 | -0,01 | -0,05 | -0,02 | -0,03 | -0,02 | 0,27 | -0,08 | 0 |
| Gp | 0,00 | 0,20 | -0,01 | 0,00 | | -0,07 | -0,02 | 0,06 | -0,02 | -0,03 | 0,09 | -0,23 | 0,03 | 0 |
| Sm | 0,00 | -0,15 | -0,02 | -0,01 | -0,02 | | -0,01 | 0,00 | 0,00 | -0,03 | 0,00 | 0,18 | 0,05 | 0 |
| Sg | -0,23 | -0,13 | -0,01 | 0,00 | -0,02 | 0,16 | | -0,05 | -0,02 | 0,30 | -0,02 | 0,11 | -0,08 | 0 |
| Sp | 0,02 | -0,13 | -0,01 | 0,00 | -0,02 | 0,11 | -0,02 | | 0,02 | 0,01 | 0,02 | 0,06 | -0,04 | 0 |
| St | -0,14 | -0,13 | -0,01 | 0,00 | -0,02 | -0,18 | -0,02 | 0,03 | | -0,03 | 0,06 | 0,52 | -0,08 | 0 |
| Sr | 0,06 | -0,13 | -0,01 | 0,00 | -0,02 | -0,12 | -0,02 | 0,01 | -0,02 | | 0,15 | 0,12 | -0,02 | 0 |
| Sh | -0,01 | -0,13 | -0,01 | 0,00 | -0,02 | 0,04 | 0,20 | -0,05 | 0,05 | 0,11 | | -0,16 | -0,01 | 0 |
| Fm | 0,09 | -0,16 | -0,02 | -0,01 | -0,02 | 0,07 | -0,02 | -0,01 | -0,01 | 0,00 | 0,00 | | 0,09 | 0 |
| Fl | 0,15 | -0,14 | -0,01 | 0,00 | -0,02 | 0,06 | 0,01 | -0,02 | -0,03 | -0,03 | -0,03 | 0,06 | | 0 |

4 and 5. Elements in the difference matrix show how many times more (+) or less (-) frequently each facies transition occurs. Geologically, it means that a facies is likely to pass upward into another facies if the corresponding difference value of their transition in the difference matrix is positive. The results of Markov Chain analysis, therefore, give the first clear impression of the possible succession of the facies in the Citalang Formation. The succession may be depicted by a facies relationship diagram (Figure 5).

Considering the facies transition as derived from the difference matrix (Table 6, Figure 5), one does not know whether a given difference is significant. The transition from facies Gmg to facies Fm in Table 6 is, for example, 0.27. Is 0.27 significant?

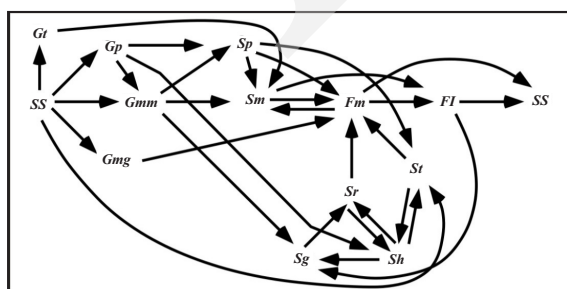


Figure 5. Facies relationship diagram of the Citalang Formation derived from the difference matrix (Table 6).

Geologically, it means that one may not be able to determine the most likely facies succession based on the difference matrix alone, as in the case of the Citalang Formation. This situation is indicated clearly from the complex form of the facies relationship diagram (Figure 5).

To cope with such a situation, Harper (1984) suggested a relatively simple method that was based on binomial probability. The following exposition on the method is paraphrased from Harper (1984):

1. Choose a level of significance α (0.10, say).
2. For each possible facies transition i to j where the difference is positive, *e.g.*, facies Gmg overlain by facies Fm, compute the probability of at least the observed number of successes (observations of Fm over Gmg) in N trials (observations of any facies other than Gmg over Gmg) given the null hypothesis that (a) the transition occurs at random, and (b) the N trials are independent.
3. Tentatively reject the null hypothesis if the probability computed in step 2 is greater or equal to the level of significance chosen. Otherwise, do not reject the null hypothesis.
4. For each possible transition where the difference is negative, proceed as above, except compute the probability of at least the observed number or fewer successes.

The probability of at least one nob transition in N trials is the binomial probability of at least one nob success in N trials, and is given by:

$$\sum_{n=n_{obs}}^{n=N} C(N,n)p^n q^{N-n} \dots\dots\dots(4)$$

where:

$C(N,n)$ = the number of possible combinations of N objects taken n at a time, and is given by:

$$C(N,n) = \frac{N!}{(N-n)!n!}$$

p = the probability of success on a single trial.

Table 7 shows the summary of binomial probability for all differences with a level of significance of 0.1. Data transitions with a probability greater than 0.15, with a level of significance $\alpha \geq 0.1$, are not listed.

Tabel 7. Binomial Probability for the Citalang Formation (Modified from Setiadi, 2001)

| Facies Transition | Binomial Probability |
|-------------------|----------------------|
| SS to Gmm | 6,22E-19 |
| SS to Gmg | 0,00703 |
| SS to Gp | 0,001 |
| Gmm to Sm | 0,00696 |
| Sm to Fm | 0,000331 |
| Sg to Sr | 0,0141 |
| St to Fm | 0,000191 |
| Sr to Sh | 0,0073 |
| Sh to Sg | 0,00109 |
| Fm to SS | 0,0312 |
| Fm to Fl | 0,00412 |
| Fl to SS | 0,0335 |

DISCUSSION

Figure 6, derived from Table 7, indicates that there are likely two lithofacies successions in the Citalang Formation. The main line of transition in the first association runs from the scoured surface (SS) through the Gmm, Sm, and Fm facies, and

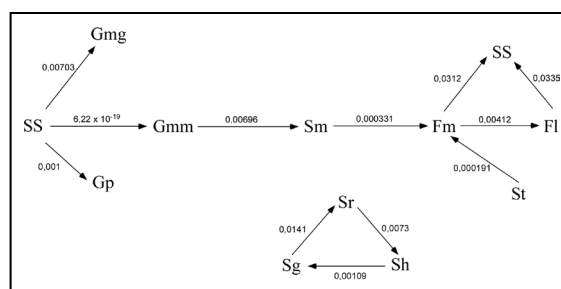


Figure 6. Facies relationship diagram for the Citalang Formation as derived from the binomial probability of Table 7 (modified from Setiadi, 2001).

topped by the Fl facies. The second association, on the other hand, shows circular transitions and is formed by the Sh, Sg, and Sr facies.

The aforementioned statistical analysis, though it successfully revealed the general patterns of facies succession, gives no clear indication of the relationships between the two successions. However, if one uses higher levels of significance, he is able to construct a more comprehensive facies relationship diagram (Figure 7), leading to the formulation of a local facies model of The Citalang Formation (Figure 8).

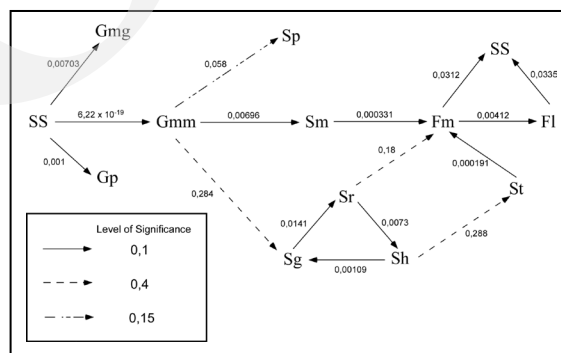


Figure 7. Facies relationship diagram for The Citalang Formation as derived from the binomial probability. Heavy lines show relationships significant at 0.1 level; dashed lines show relationships significant at 0.4 level, except the transition Gmm → Sp that is significant at 0.15 level (modified from Setiadi, 2001).

The facies model of the Citalang Formation consists of two components. The first component—which is composed of the SS, Gmm, Sm, Sp, St, Fm, and Fl lithofacies—is referred to in this thesis as the fining-upward succession, because it shows a general trend of fining-up of

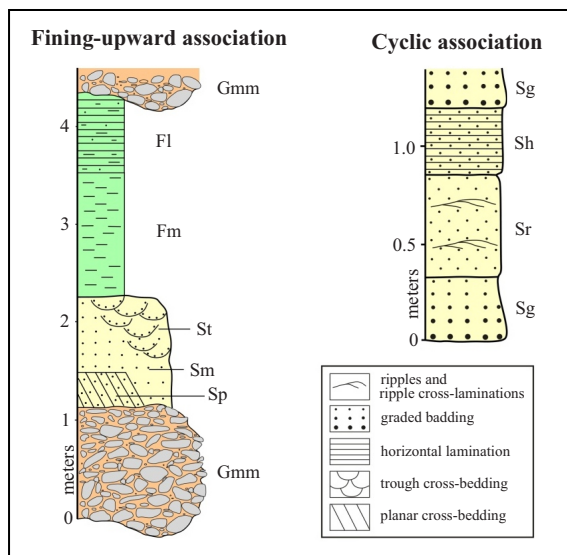


Figure 8. A facies model of the Citalang Formation (Setiadi, 1998).

grain size (Figure 8). As indicated by the results of statistical analysis (Figure 6; Tables 6 and 7), the lithofacies Gmg, Gt, and Gp also belong to this association. They are not included in the facies model, because they are regarded as incidental members of this association since they have no statistically significant relationship to the sandy facies. The second component—which is composed of the Sg, Sh, and Sr lithofacies—is referred to as the cyclic association, because it shows a cyclic character.

Statistically, both of the aforementioned associations in the local facies model of the Citalang Formation may connect to each other through the $Gmm \rightarrow Sg$ and $Sr \rightarrow Fm$ transitions. The relationship has a 0.4 level of significance, because they have binomial probability of 0.284 and 0.180, respectively.

By considering the characters of all facies, their relationships as revealed from statistical analysis, and by comparison with a suitable general facies model (Figure 8), the fining-upward sequence has been interpreted as a sequence of channel-bar-overbank deposits developed in the vicinity of a braided stream channel system (Setiadi, 1998). The Citalang Formation, therefore, may overall represent a braided stream deposit (Setiadi, 1998, 2001).

The presence of channel-bars and floodplain fines, on the other hand, is a typical feature observed in fluvial systems, and the presence of facies was determined in this study based on the level of significance as well. Channel-bars may be coupled with avulsion on a broader scale, which is often present in many fluvial depositional systems as an alternation between avulsion and overbank deposits. Given that no considerable thickness was observed in the facies, subsidence may have played a minor impact in the creation of fluvial facies in the Citalang Formation. The occurrence of cyclic association facies, which The Markov Chain approach successfully revealed, could be a subject of concern for external orbital forcing. However, the orbital forcing scale that regulates the cyclic association in the Citalang Formation, whether precession, obliquity, or eccentricity, is sometimes a controlling variable for sedimentation in the fluvial system, in which no evidence of sea-level influence was identified.

CONCLUSIONS

The successful application to real-world geologic materials, such as the Citalang Formation described in this paper, suggests that a combination of the embedded Markov Chain and binomial probability can be used to analyze sedimentary facies.

The method should be considered as a means of achieving unbiased results or, at the very least, constraining geological interpretation of relationships between observable facies that are not easily (or, more often, very difficult) to perceive physically from stratigraphic sections.

Acknowledgments

The authors are grateful to Dr. Nurdrajat and Dr. Billy G. Adhiperdhana from the Faculty of Geological Engineering, Padjadjaran University, for their encouragement and constructive comments on various drafts of the paper. The authors have no conflicts of interest.

REFERENCES

- Alam, S., Sendjaja, Y.A., Jurnaliah, L., Gani, R.M.G., and Fachrudin, A., 2019. Evidence of Pliocene-Pleistocene Unconformity in Eastern Bogor Trough, Sumedang-West Java. *Journal of Geological Sciences and Applied Geology*, 3 (1), p.38-43.
- Cant, D.J. and Walker, R.G., 1976. Development of a braided fluvial facies model for the Devonian Battery Point sandstone, Quebec. *Canadian Journal of Earth Sciences*, 13, p.102-119. DOI: 10.1139/e76-010
- Catuneanu, O., 2006. *Principles of Sequence Stratigraphy*. Elsevier B.V.
- Colombera, L., Mountney, N.P., and McCaffrey, W.D., 2013. A quantitative approach to fluvial facies models: Methods and example results. *Sedimentology*, 60 (6), p.1526-1558. DOI: 10.1111/sed.12050
- Croix, L., He, J., Wang, J., and Underschultz, J., 2019. *Facies prediction from well logs in the Precipice Sandstone and Evergreen Formation in the Surat Basin, The University of Queensland Surat Deep Aquifer Appraisal Project-Supplementary Detailed Report*.
- Dalrymple, R.W., 2010. Interpreting sedimentary successions: Facies, facies analysis, and facies models. In: *Facies Models* (4th ed., p.3-18). St. John's: Geological Association of Canada. DOI: 10.1002/9781444304091.ch7
- Djuri, 1973. Geological map of the Arjawinangun Quadrangle, Jawa, scala 1:100.000. Geological Research and Development Centre, Bandung
- Dyer, B., Maloof, A.C., Purkis, S.J., and Harris, P.M., 2018. Quantifying the relationship between water depth and carbonate facies. *Sedimentary Geology*, 373, p.1-10.
- Gingerich, P.D., 1969. Markov analysis of cyclic alluvial sediments. *Journal of Sedimentary Petrology*, 39, p.330-332.
- Harms, J.C., Southard, J.B., Spearing, D.R., and Walker, R.G., 1975. Depositional Environments as Interpreted from Primary Sedimentary Structures and Stratification Sequences. *SEPM Short Course Note 2*, 161pp. DOI: 10.2110/scn.75.01.0133
- Harper, C.W.J., 1984. Improved methods of facies sequence analysis. In: *Facies Models* (2nd ed., p.11-13). Geological Society of Canada.
- He, J., La Croix, A.D., Wang, J., Ding, W., and Underschultz, J.R., 2019. Using neural networks and the Markov chain approach for facies analysis and prediction from well logs in the Precipe Sandstone and Evergreen Formation, Surat Basin, Australia. *Marine and Petroleum Geology*, 101, p.410-427.
- Hota, R.N. and Das, B.K., 2010. Cyclic sedimentation of the Barren Measures Formation (Damuda Group), Talchir Gondwana Basin: Statistical appraisal from borehole logs. *Journal of the Geological Society of India*, 75, p.549-559. DOI: 10.1007/s12594-010-0044-6
- Hsieh, A.I., Allen, D.M., and MacEachern, J.A., 2015. Statistical modeling of biogenically enhanced permeability in tight reservoir rock. *Marine and Petroleum Geology*, 65, p.114-125.
- Kazi-Tani, L.M. and Gaouar, A., 2016. An application of embedded Markov chain for soil sequences: Case study in north western part of Algria. *Eurasian Journal of Soil Science*, 5, p.231-240. DOI: 10.18393/ejss.2016.3.231-240
- Lapcik, P., 2019. Facies anatomy of a progradational submarine channelized lobe complex: Semiquantitative analysis of the Ropianka Formation (Campanian-Paleocene) in Hucisko Jawornickie section, Skole Nappe, Polish Carpathians. *Acta Geologica Polonica*, 69, p.111-141.
- Li, P., Kneller, B., Thompson, P., Bozetti, G., and Santos, T., 2018. Architectural and facies organisation of slope channel fills: Upper Cretaceous Rosario Formation, Baja California, Mexico. *Marine and Petroleum Geology*, 92, p.632-649.
- Li, W., Zhang, C., Burt, J.E., and Zhu, A.X., 2005. A Markov-chain based probability vector approach for modeling spatial uncertainties of soil classes. *Soil Science Society of America Journal*, 68, p.1931-1942. DOI: 10.2136/sssaj2004.0258a
- Lindholm, R., 1987. *A Practical Approach to Sedimentology*. Allend & Unwin, 279pp.

- Marino, J.E. and Amaya, E., 2016. Lithofacies cyclicity determination in the Guaduas Formation (Colombia) using Markov chains. *Earth Sciences Research Journal*, 20 (3), B1-B9. DOI: 10.15446/esrj.v20n3.44429. DOI: 10.15446/esrj.v20n3.44429
- Miall, A.D., 1973. Markov chain analysis applied to an ancient alluvial plain succession. *Sedimentology*, 20, p.347-364.
- Miall, A.D., 1985. Architectural-element analysis: A new method of facies analysis applied to fluvial deposits. *Earth Science Reviews*, 22, p.261-308.
- Miall, A.D., 2016. *Stratigraphy: A Modern Synthesis*. Cham: Springer, 464pp.
- Milo, S.P., 2017. *Detection of Sedimentary Depositional Cycles in the Salado Formation, Southeastern New Mexico*. University of Mississippi.
- Pérez-Pueyo, M., Bádenas, B., and Villas, E., 2018. Sedimentology and paleontology of the lower member of the Nogueiras Fm (Lower Devonian) at Santa Cruz de Noguearas (Teruel, NE Spain). *Revista de La Sociedad Geologica de España*, 31, p.89-104.
- Pirrie, D., 1998. Interpreting the record: Facies analysis. In: *Unlocking the Stratigraphical Record: Advances in Modern Stratigraphy*, p.395-420. Chichester: John Wiley & Sons.
- Reineck, H.E. and Singh, I.B., 1980. *Depositional Sedimentary Environments* (2nd ed.). Springer-Verlag, 549pp. DOI: 10.1007/978-3-642-81498-3
- Scholle, P.A., Bebout, D.G., and Moore, C.H., 1983. Carbonate Depositional Environments. *American Association of Petroleum Geologists Memoir*, 33, 708pp. DOI: 10.1306/m33429
- Scholle, P.A. and Spearing, D., 1982. Sandstone Depositional Environments. *American Association of Petroleum Geologists Memoir*, 31, 410pp.
- Selley, R.C., 1969. Studies of sequences in sediments using a simple mathematical device. *Quarterly Journal of the Geological Society of London*, 125, p.557-581. DOI: 10.1144/gsjgs.125.1.0557
- Setiadi, D.J., 1998. *Lithofacies and Depositional Environments of the Citalang Formation, West Java, Indonesia*. Osaka City University, Japan.
- Setiadi, D.J., 2001. Fluvial facies of The Citalang Formation (Pliocene–Early Pleistocene), West Java, Indonesia. *Journal of Geosciences, Osaka City University*, 44, p.189-199.
- Silitonga, P.H., 1973. Geological Map of the Bandung Quadrangle, Jawa, scale 1:100.000. Geological Research and Development Centre, Bandung
- Soto, M.B., Durán, E.L., and Aldana, M., 2014. Stratigraphic columns modeling and cyclicity analysis of the Misoa Formation, Maracaibo Lake, Venezuela, using Markov chain. *Geofisica Internacional*, 53, p.277-288. DOI: 10.1016/s0016-7169(14)71505-3
- Stanova, S., Sotak, J., and Hudec, N., 2009. Markov chain analysis of turbiditic facies and flow dynamics (Magura Zone, Outer Western Carpathians, NW Slovakia). *Geologica Carpathica*, 60 (4), p.295-305.
- Subagja, M.A., Setiadi, D.J., Jurnaliah, L., Syafri, I., Alam, S., and Elfitra, D., 2019. Pendekatan kuantitatif dalam penentuan asosiasi Fasies Laut Dalam Formasi Halang pada Sungai Kaligintung, Jawa Tengah. *Bulletin of Scientific Contribution, Universitas Padjadjaran*, 17 (3), p.193-204.
- Sumner, E.J., Talling, P.J., Amy, L.A., Wynn, R.B., Stevenson, C., and Frenz, M., 2012. Facies architecture of individual basin-plain turbidites: Comparison with existing models and implications for flow processes. *Sedimentology*, 59 (6), p.1850-1887. DOI: 10.1111/j.1365-3091.2012.01329.x
- Tewari, R.C. and Khan, Z.A., 2017. Structures and sequence in early Permian fluvial Barakar rocks of peninsular India Gondwana basins using binomial and Markov chain analysis. *Arabian Journal of Geosciences*, 10, p.1-15. DOI: 10.1007/s12517-016-2799-6
- Walker, R.G., 1984. *Facies Models* (2nd ed.). Geological Society of Canada.
- Walker, R.G. and James, N.P., 1992. *Facies Models: Response to Sea Level Change*. Geological Society of Canada.